

Unitary Selective Coupled-Cluster Method

Dmitry A. Fedorov,^{†,‡} Yuri Alexeev,[†] Stephen K. Gray,[¶] and Matthew Otten^{*,§}

[†]*Computational Science Division, Argonne National Laboratory, 9700 S. Cass Ave.,
Lemont, IL 60439, USA*

[‡]*Oak Ridge Associated Universities, Oak Ridge, TN 37830*

[¶]*Center for Nanoscale Materials, Argonne National Laboratory, 9700 S. Cass Ave.,
Lemont, IL 60439, USA*

[§]*HRL Laboratories, LLC, 3011 Malibu Canyon Road, Malibu, CA 90265*

E-mail: mjotten@hrl.com

Abstract

Simulating molecules using the Variational Quantum Eigensolver method is one of the promising applications for NISQ-era quantum computers. Designing an efficient ansatz to represent the electronic wave function is crucial in such simulations. In this work we present a method that allows a significant reduction of the size of the unitary coupled cluster with singles and doubles (UCCSD) ansatz at zero cost. This method uses the electronic Hamiltonian matrix elements to filter out excitations for which such matrix elements are zero. For symmetric molecules, this method can achieve reductions of up to five times for a minimal basis set, and this reduction factor increases for larger basis sets. We also propose a more general unitary selective coupled-cluster method, a way to construct a unitary coupled-cluster ansatz with excitations up to fourth order using a selection procedure. This approach uses the electronic Hamiltonian matrix elements and the amplitudes for excitations already present in the ansatz to find the important excitations of higher order and to add them to the ansatz. The important

feature of the method is that it systematically reduces the energy error with increasing ansatz size for a set of test molecules.

Introduction

One of the promising and natural applications of quantum computers is the simulation of quantum systems. By representing a state of a quantum system on a quantum computer, one can, in theory, avoid the exponential scaling faced on classical computers when manipulating the state of a quantum system. For example, it has been proven that the quantum phase estimation (QPE) algorithm can find eigenvalues of unitary operators exponentially faster than a classical computer can.¹⁻³ Since the time propagator of a quantum system is a unitary operator, QPE seems like a good candidate for solving many problems from physics and chemistry on quantum computers. However, running such simulations is far beyond the capabilities of current, noisy intermediate-scale quantum (NISQ) hardware.^{4,5} The Variational Quantum Eigensolver (VQE)⁶ is a hybrid quantum-classical algorithm to find eigenvalues of molecular Hamiltonians that requires shallower circuits than QPE. The shallower circuits are achieved at the expense of a larger number of measurements and by offloading a part of the computational workload onto a classical computer. In VQE simulations, it is important to choose an efficient variational ansatz that (a) is expressible enough so that it can represent a good solution to the problem, (b) is not too expressible so that the solution space is limited to relevant parts of Hilbert space, (c) does not have too many parameters to optimize, and (d) can be represented by short circuits.⁷

Conceptually, one can approach the problem of designing a variational ansatz in two ways. The first, so-called chemistry-inspired type of ansatzes, is based on the unitary coupled-cluster (UCC) method. The unitary coupled cluster with singles and doubles (UCCSD)⁸⁻¹² ansatz was used to run the first VQE simulation.^{6,13,14} This ansatz is inspired by the commonly used classical coupled-cluster method. Essentially, each parameter in a UCCSD ansatz

parameterizes a coupled-cluster amplitude for each fermionic excitation from a reference state, either a single or a double excitation. This ansatz has been successfully applied to compute accurate electronic energies of small molecules. Because of the physically motivated structure, it is usually easy to optimize such ansatzes because they generate states that correspond to realistic electronic wave functions. However, such ansatzes for a large molecule can have many redundant, unimportant excitations and, therefore, a large number of parameters to optimize and excessively long circuits. This problem occurs because the only variables used when generating an ansatz are the number of orbitals and electrons, without taking into account the information about the specific chemical system, such as geometry.

The second group of ansatzes is called "hardware-efficient." Such ansatzes contain sequences of parameterized single- and two-qubit gates that can be easily implemented on the quantum computer at hand.¹⁵⁻¹⁹ No information about the physics of the molecule being studied is used. Hardware-efficient ansatzes are usually very expressible. Furthermore, the circuits to implement them are shallower compared with UCCSD ones and contain a smaller number of error-prone two-qubit quantum gates. However, such ansatzes can also have too many parameters to optimize and suffer from the "barren plateaus"²⁰⁻²² problem. In addition, because of the lack of physically motivated structure, extra work needs to be done to enforce physical symmetries, such as antisymmetry of the wave function and particle number.¹⁹

A number of recent studies have focused on designing ansatzes iteratively by adding elements into the ansatz based on some system-specific criterion compared with a general-purpose ansatz such as UCCSD..²³⁻²⁹ The first iterative algorithm, ADAPT-VQE,²³ adds fermionic operators to the ansatz based on the gradient. The choice of an operator to add at each step is performed by computing the energy gradients with respect to variational parameters. This screening procedure allows one to pick operators that will contribute the most to the lowering of energy. The criterion to choose the operators is borrowed from the anti-Hermitian contracted Schrödinger equation methodology.³⁰⁻³⁴ In a variation of the ADAPT-

VQE method, called qubit-ADAPT-VQE,²⁴ the fermionic operators are broken down into Pauli strings and used as building blocks for constructing an ansatz. As a result, the circuits have fewer two-qubit gates, which makes this ansatz more NISQ-friendly. However, the number of variational parameters is significantly larger than in ADAPT-VQE, which makes classical optimization harder and increases the number of ADAPT iterations. Yordanov et al.³⁵ proposed to use so-called qubit excitations³⁶ instead of the fermionic excitations in ADAPT-VQE simulations. Qubit excitation operators are simply fermionic excitations with the products of Pauli-Z operators removed. These Pauli-Z operators are responsible for preserving the antisymmetry of the wave function. This greatly simplifies the problem due to the absence of cascades of two-qubit gates, which means that every excitation operator can be implemented by using a constant number of CNOT gates, unlike fermionic excitation operators, in which the number of CNOTs scales linearly with the number of qubits. Numerical simulations on small molecules showed that the lack of antisymmetry is compensated by the flexibility of the variational ansatz. However, such an approach still needs to be validated on larger systems.

In the qubit coupled-cluster (QCC)²⁵ method and its iterative version²⁶ the ansatz is constructed directly in the qubit space. Similar to ADAPT-VQE, the decision on which operator to add to the ansatz is based on the gradients of energy with respect to variational parameters corresponding to these operators.

An alternative way to increase the efficiency of a fermionic operator-based ansatz is to use the prescreening procedure based on the t_2 amplitudes, coefficients computed by using Møller-Plesset second-order perturbation (MP2) theory,^{37,38} corresponding to double-excitation fermionic operators. MP2 amplitudes are routinely used as an initial guess for CCSD amplitudes in the classical CCSD simulations. Although MP2 calculations require significant computational effort with $O(N^5)$ asymptotic scaling, they can significantly improve CCSD convergence and result in overall time savings. This approach can be directly applied to UCCSD, where MP2 amplitude screening can reduce the number of excitation

operators in the ansatz and significantly reduce the quantum gate count for certain molecular systems.¹⁴

VQE-UCC Framework

We begin with a brief introduction to the VQE method and the UCC ansatz, which is necessary for understanding the rest of this work. A more detailed description can be found in several recent, comprehensive reviews.^{39–42} The goal is to solve the time-independent Schrödinger equation for electrons, which is obtained by applying the Born–Oppenheimer approximation for separation of electronic and nuclear degrees of freedom. This equation is an eigenvalue problem $H_{el} |\psi\rangle = E |\psi\rangle$, where $|\psi\rangle$ is the electronic wave function, E is the energy of the ground electronic state, and H_{el} is an electronic Hamiltonian, which can be written by using the second quantization formalism as

$$H_{el} = \sum_{pq}^{N_{MO}} h_{pq} a_p^\dagger a_q + \sum_{pqrs}^{N_{MO}} h_{pqrs} a_p^\dagger a_q^\dagger a_s a_r. \quad (1)$$

In Equation 1, indices p , q , r , and s denote the molecular spin orbitals, N_{MO} is the total number of molecular spin orbitals, and h_{pq} and h_{pqrs} are the electronic Hamiltonian matrix elements connecting corresponding spin orbitals. These electronic Hamiltonian matrix elements are also referred to as one- and two-electron integrals. We will use the two terms interchangeably throughout the paper. Here a_p^\dagger and a_q are creation and annihilation operators, respectively, which add or remove an electron from orbitals p and q . The second-quantized fermionic Hamiltonian can be mapped onto the qubit space by using one of the fermion-to-qubit mappings. In the current work we employ the Jordan–Wigner mapping,⁴³ which has an important benefit: molecular spin-orbital occupation numbers 0, 1 directly map onto the

qubit states 0, 1. The resulting qubit Hamiltonian takes the form

$$H = \sum_j \alpha_j P_j = \sum_j \alpha_j \prod_i \sigma_i^j, \quad (2)$$

where α_j are coefficients that depend on electron integrals h_{pq} and h_{pqrs} . Each Pauli string P_j is a product of Pauli matrices $\sigma_i^j \in (I, X, Y, Z)$. Index i denotes the qubit that the Pauli operator acts on, and j denotes the term of the qubit Hamiltonian. After preparing the Hamiltonian, one has to choose the trial wave function $|\psi(\vec{t})\rangle$ form to measure the energy of the system on a quantum computer,

$$E(\vec{t}) = \sum_j \alpha_j \langle \psi(\vec{t}) | \prod_i \sigma_i^j | \psi(\vec{t}) \rangle. \quad (3)$$

The variational parameters \vec{t} can be optimized on a classical computer by using conventional optimization techniques to minimize the energy, relying on the Rayleigh–Ritz variational principle:

$$E \leq \frac{\langle \psi(\vec{t}) | \hat{H}_{el} | \psi(\vec{t}) \rangle}{\langle \psi(\vec{t}) | \psi(\vec{t}) \rangle}. \quad (4)$$

Because of the stochastic nature of the quantum measurements, the energy in this equation has to be measured multiple times to gather statistics and reduce the error. This process is called Hamiltonian averaging.⁴⁴

In this study we work with the unitary coupled-cluster (UCC) ansatz, which, as noted above, is a so-called chemistry-inspired ansatz. It is a unitary version of the classical coupled-cluster method, a high-accuracy method in classical quantum chemistry.⁴⁵ Unlike the regular coupled-cluster (CC) theory, however, UCC can be efficiently implemented on a quantum computer. The wave function is parameterized by using a unitary operator,

$$|\psi(\vec{t})\rangle = e^{\hat{T}-\hat{T}^\dagger} |\phi\rangle, \quad (5)$$

where \hat{T} is the cluster excitation operator. Since including all possible excitations is not computationally feasible because of exponential scaling with system size, the CC expansion is truncated, most commonly at the doubles level, which corresponds to the UCCSD ansatz

$$\hat{T} = \hat{T}_1 + \hat{T}_2 = \sum_{i \in \text{virt}, a \in \text{occ}} \hat{t}_i^a + \sum_{i, j \in \text{virt}, a, b \in \text{occ}} \hat{t}_{ij}^{ab} = \sum_{i \in \text{virt}, a \in \text{occ}} t_i^a \hat{a}_i^\dagger \hat{a}_a + \sum_{i, j \in \text{virt}, a, b \in \text{occ}} t_{ij}^{ab} \hat{a}_i^\dagger \hat{a}_j^\dagger \hat{a}_a \hat{a}_b. \quad (6)$$

Each fermionic excitation operator included in the UCCSD ansatz is an exponentiated anti-Hermitian sum of excitation and de-excitation operators represented by the unitary

$$\hat{A}_i^a(t_i^a) = \exp \left[t_i^a (a_i^\dagger a_a - a_a^\dagger a_i) \right] \quad (7)$$

$$\hat{A}_{ij}^{ab}(t_{ij}^{ab}) = \exp \left[t_{ij}^{ab} (a_i^\dagger a_j^\dagger a_b a_a - a_a^\dagger a_b^\dagger a_j a_i) \right], \quad (8)$$

where t_i^a and t_{ij}^{ab} are the cluster amplitudes, each corresponding to an excitation from occupied orbitals i and j into virtual orbitals a and b . The direct implementation of such an exponential operator with many terms that act on all qubits is not possible on quantum hardware. The operator needs to be broken into a sequence of operators acting on a few qubits each. Trotterization using the Suzuki–Trotter expansion⁴⁶ is the most common approach to achieve this goal and is defined as

$$e^{A+B} = \lim_{n \rightarrow \infty} (e^{A/n} e^{B/n})^n. \quad (9)$$

Because of the variational flexibility of the UCC ansatz, the Trotter error usually remains small even if a single Trotter step ($n = 1$) is used.⁴⁷

These cluster amplitudes t_i^a and t_{ij}^{ab} are the direct analogs of the cluster amplitudes in the classical CCSD method. In UCCSD, amplitudes are variationally optimized in a classical loop during a VQE simulation, and generally UCCSD amplitudes are different from CCSD ones. Although all generated ansatz elements are inspired by chemistry, with a single parameter that controls the contribution of a particular excitation, the UCC ansatz has a

drawback that can make it inefficient for large systems. Specifically, the UCC ansatz depends only on the number of molecular orbitals and electrons; it does not take into account the information about the chemistry of the particular molecule. For example, different molecules will have different sets of important excitations. As a result, the UCC ansatz can contain a large fraction of excitations that are insignificant or are simply zero because of the presence of symmetry. Since implementing each excitation on quantum hardware is expensive and the total number of possible excitations grows rapidly with system size, considerable effort has been expended in designing more efficient UCC ansatzes. The focus of this work is on constructing an efficient UCC ansatz that includes the “most important” fermionic excitation operators that contribute the most to the correlation energy.

Selected CI

Within classical algorithms for quantum chemistry there exist many techniques for calculating estimates of the ground state energy, including the coupled-cluster methods (such as CCSD) mentioned above.⁴⁵ Another family of algorithms works in the determinant basis, rather than with cluster operators. Full configuration interaction (FCI) finds the coefficients of the combinatorially many determinants of the many-body wave function through an exact diagonalization-like approach.⁴⁸ Similar to the discussion of the drawbacks of the UCC above, often many of the FCI coefficients are small, or even zero, leading to a large amount of excess computation. One way of reducing the exponential scaling is to include determinants only up to some order; the configuration interaction singles and doubles (CISD) wave function, for instance, truncates the space by including only determinants that are a single or double excitation from the reference state (typically, the Hartree–Fock state).⁴⁹ For many systems with correlation, this is not sufficient to have an accurate description of the wave function. Selective configuration interaction algorithms, such as perturbatively selected configuration interaction (CIPSI),⁵⁰ adaptive sampling configuration interaction (ASCI),⁵¹

and selected heat-bath configuration interaction (SHCI),^{52,53} use an iterative procedure to select only important determinants to include in the wave function, regardless of the order of excitation. These methods also typically include a second-order perturbation theory step to provide additional accuracy. Although this is still exponentially scaling, it often leads to a dramatic reduction in the number of determinants needed to reach accurate calculations, allowing for FCI-quality energies in systems as large as the highly correlated chromium dimer, correlating 28 electrons in 198 orbitals (a Hilbert space of size $\approx 10^{42}$).⁵⁴ SCI methods can also be used to find excited states, through a modified selection criterion.^{55,56}

Here, we briefly review the determinant selection step of the SHCI algorithm, since some of its features inspired the unitary selected coupled-cluster algorithm that we discuss below. A more complete description of the SCHI algorithm can be found in Refs.^{52,53} In the variational step of SHCI, determinants connected to the current variational set of determinants \mathcal{V} (which, at the first iteration, is typically just the Hartree–Fock determinant) are screened for importance via the selection criterion

$$\max_{D_i \in \mathcal{V}} |H_{ia}c_i| > \epsilon_1, \quad (10)$$

where H_{ia} is the Hamiltonian matrix element connecting determinant D_a , which is not currently in the variational set \mathcal{V} , to determinant D_i , which is currently in the variational set with coefficient c_i . Here ϵ_1 is a user-defined cutoff that controls the accuracy of the method; in the limit that ϵ_1 is 0, the method will include all determinants and is equivalent to FCI. Other SCI methods, such as CIPSI,⁵⁰ use a selection criterion based on perturbation theory. The SHCI selection criterion has the intuitive interpretation of being the “most important” part of the perturbative correction.⁵² It can also be interpreted, loosely, as including determinants that are strongly connected (having a large matrix element H_{ia}) to an important determinant (one that has a large coefficient, c_i).

Fermionic Operator Prescreening

The prescreening procedure for fermionic excitation operators described in this section is inspired by the selected CI algorithm,,⁵⁷ which, as discussed above, uses electronic Hamiltonian matrix elements to find determinants that have the potential to contribute the most to the correlation energy. In this work we use these electronic Hamiltonian matrix elements to find the excitation operators that have a negligible contribution to the correlation energy. To demonstrate this method, we chose the H_4 molecule, which is an appropriate system for benchmarking. On the one hand, it is small, with only 4 electrons over 8 spin orbitals. On the other hand, it has a significant amount of correlation energy at stretched geometries. A well-known approach to prescreen the CC amplitudes is to use MP2 amplitudes. Romero et al.¹⁴ performed a systematic study of the H_4 molecule, where the energies were computed for different geometric configurations of the molecule using the VQE method and UCCSD ansatz with the excitation operators for UCCSD prescreened with different MP2 amplitude thresholds. The results showed that the number of operators in the ansatz was reduced by up to a factor of 3 for some geometries without sacrificing accuracy.

In the minimal STO-3G basis set, the H_4 molecule has 26 excitations up to the second order: 8 singles and 18 doubles. We first consider the symmetric linear chain with equal H-H bond distances. In Figure 1(a) we plot the values of electronic Hamiltonian matrix elements connecting the occupied spin orbitals i, j with virtual spin orbitals a, b for $R_{H-H} = 1.5 \text{ \AA}$. Figure 1(b) depicts the t_1 and t_2 CCSD amplitudes connecting the same spin orbitals. The excitations are written in spin-block notation: the occupied orbitals, from which excitations are performed, are labeled i, j, k , and l ; and the virtual orbitals, to which electrons are excited, are labeled a, b, c , and d . For example, single and double excitations are written as $[i, a]$ and $[i, j, a, b]$. The electron integrals between these orbitals are respectively $h_1[i, a]$ and $h_2[i, j, a, b]$. For the symmetric configuration represented by the blue bars, one can immediately notice that the excitations for which electronic Hamiltonian matrix elements are zero also have zero CCSD amplitudes. To check whether this relation stands for differ-

ent geometries, we performed a classical CCSD computation of the whole potential energy surface (PES), from $R_{H-H} = 0.5 \text{ \AA}$ to $R_{H-H} = 3.0 \text{ \AA}$. The results show that it is the case. Across the whole PES, out of 8 t_1 amplitudes, 4 are negligibly small; and out of 18 t_2 amplitudes, only 10 are significant. We then computed the same PES using the VQE method and UCCSD ansatz. The VQE simulation results are consistent with CCSD and show that the excitations corresponding to the zero electronic Hamiltonian matrix elements have variational parameters converging to zero. We removed those excitations from the UCCSD ansatz and repeated the simulations with the truncated ansatz. The truncation threshold for the electron integral value was set to 10^{-8} . The UCCSD simulations with 14 out of all possible 26 single and double excitations screened by electron integrals result in the same energies and variational parameters as in the results using the full ansatz with 26 operators. Figure 3(a) shows the energy error with respect to FCI across the whole PES computed by using the full UCCSD ansatz and the prescreened ansatz. Two pairs of lines correspond to calculations performed by using Trotterization with a single step and using the direct cluster operator exponentiation. The maximum errors between the full UCCSD ansatz and the prescreened one are in Table 1. For the linear H_4 symmetric molecule, these errors do not exceed 0.0066 mHa for direct exponentiation simulations and 0.0232 mHa for Trotterized simulations. Thus, removing 12 out of 26 operators from the UCCSD ansatz does not significantly affect the accuracy, and the discrepancy that exists between full vs. prescreened ansatz is due to imperfect optimization. The differences between Trotterized and exponentiated results for larger internuclear distances we attribute to the Trotterization error.

In the broken symmetry configuration represented by orange bars in Figure 1, we adjust one of the internuclear distances $R(H_3 - H_4)$ to $0.9R$. The electron integrals and CC amplitudes that were nearly zero in the symmetric configuration now have nonzero values. Although the magnitude of the amplitudes is smaller than the amplitudes of the excitations in the symmetric version, they cannot be neglected without sacrificing accuracy. Including

only 14 excitations prescreened from the symmetric configuration results in an additional error of 4.1 mHa above the energy obtained with the full UCCSD ansatz. This observation suggests that the CCSD amplitudes and electronic Hamiltonian matrix elements are zero for some excitations because of the symmetry. This also points to the potentially poor transferability of truncated ansatzes between different molecular geometries.

In a symmetric rectangular configuration of the H_4 molecule with $R = 1.5 \text{ \AA}$, $d_1 = d_2 = 2.0 \text{ \AA}$ internuclear distances, all of the t_1 CCSD amplitudes are zero, and only 10 t_2 amplitudes are nonzero. Similarly to the linear system, the corresponding electron integrals matrix elements are zero as well (see Figure 2). The removal of these zero excitations does not affect the energy (see Figure 3(b)). For a distorted geometry with $R_{\text{H-H}} = 1.5 \text{ \AA}$, $d_1 = 2.0 \text{ \AA}$, $d_2 = 1.9 \text{ \AA}$ many more excitations have to be included similarly to the linear configurations. Including only 10 excitations prescreened from the symmetric configuration results in additional error of 0.1 mHa above energy obtained with the full UCCSD ansatz.

To confirm that the prescreening procedure works for different systems, we performed the same simulations as we did for the H_4 molecule for a set of symmetric molecules. The resulting energy errors w.r.t. FCI are presented in Figure 3. As expected, UCCSD performs well around the equilibrium distance, with errors below the chemical accuracy threshold for all considered molecules (Figure 3). At larger equilibrium distances, however, when the amount of correlation energy increases drastically, single and double excitations alone are not enough for accurate energy computation—with the exception of the LiH molecule where higher-order excitations are not contributing significantly. In addition, for larger internuclear distances, the discrepancies between the exponentiated and Trotterized simulations are observed due to the Trotterization error. For all considered molecules, however, the difference in energies between UCCSD and the truncated ansatzes does not exceed 0.023 mHa in simulations using Trotterization and 0.011 mHa in simulations using operator exponentiation. The reduction in the number of parameters ranges from 46% for the linear H_4 to 81% for the BeH_2 molecule.

These results suggest that values of electron integrals can be used for prescreening of

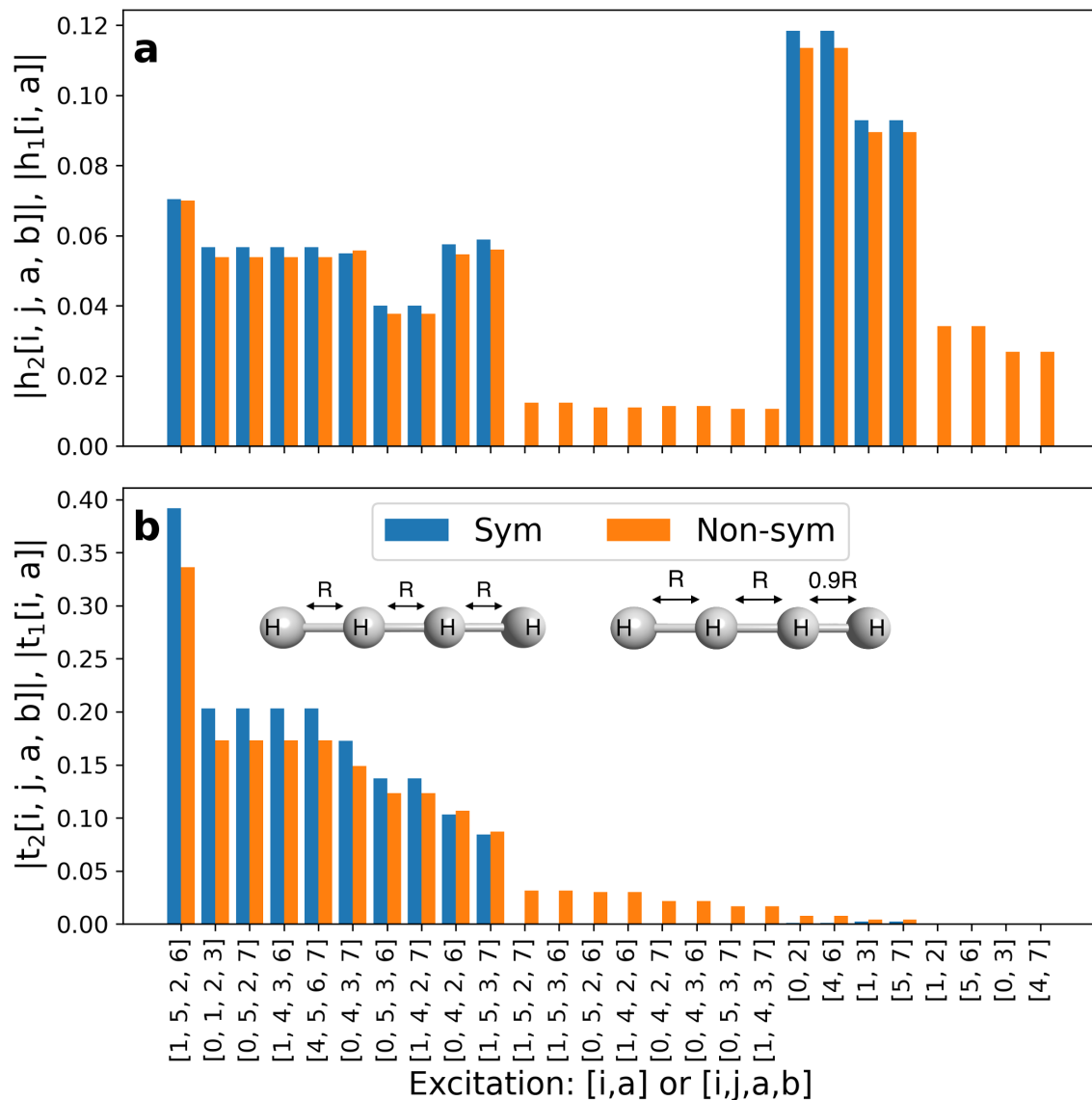


Figure 1: (a) Values of one- and two-electron integral matrix elements for the symmetric linear H_4 molecule with $R_{H-H} = 1.5 \text{ \AA}$ and the non-symmetric linear configuration with $R_{H_3-H_4} = 0.9R$. Here $h_2[i, j, a, b]$ correspond to double excitations from spin orbitals i, j to spin orbitals a, b ; and $h_1[i, a]$ correspond to single excitations from spin orbital i to spin orbital a . (b) Values of CCSD amplitudes $t_1[i, a]$ $t_2[i, j, a, b]$ for the symmetric linear H_4 molecule with $R = 1.5 \text{ \AA}$ and the non-symmetric linear configuration with $R_{H_3-H_4} = 0.9R$.

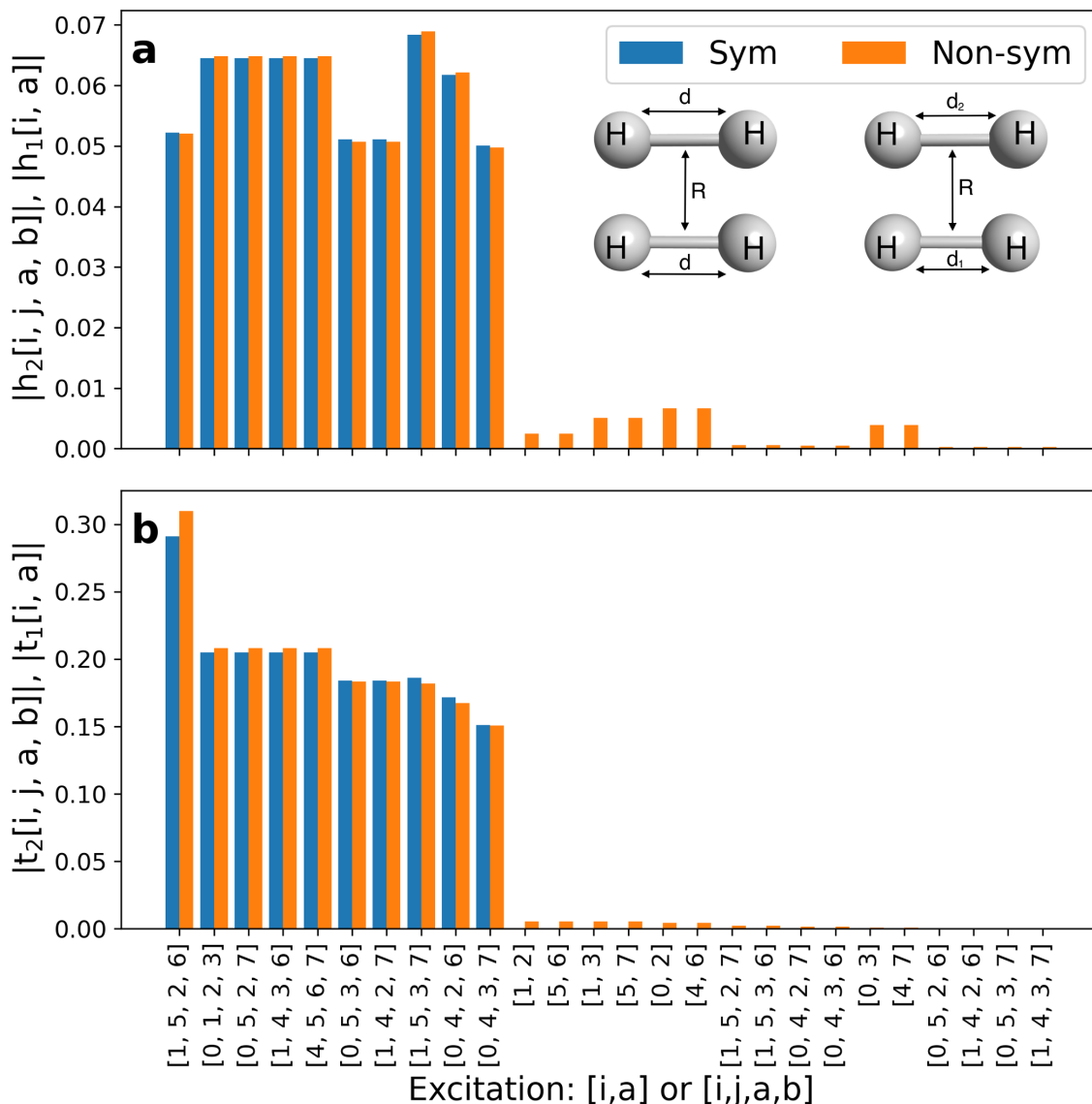


Figure 2: (a) Values of two-electron integral matrix elements $h_2[i, j, a, b]$ corresponding to double excitations $[i, j, a, b]$ for the symmetric rectangular H_4 molecule with $R = 1.5 \text{ \AA}$ and $d_1 = d_2 = 2.0 \text{ \AA}$ and the non-symmetric rectangular configuration with $R = 1.5 \text{ \AA}$, $d_1 = 2.0 \text{ \AA}$, $d_2 = 1.9 \text{ \AA}$. (b) Values of CCSD amplitudes $t_2[i, j, a, b]$ corresponding to double excitations $[i, j, a, b]$ for the symmetric rectangular H_4 molecule with $R = 1.5 \text{ \AA}$, $d_1 = d_2 = 2.0 \text{ \AA}$ and the non-symmetric square configuration with $R = 1.5 \text{ \AA}$, $d_1 = 2.0 \text{ \AA}$, $d_2 = 1.9 \text{ \AA}$

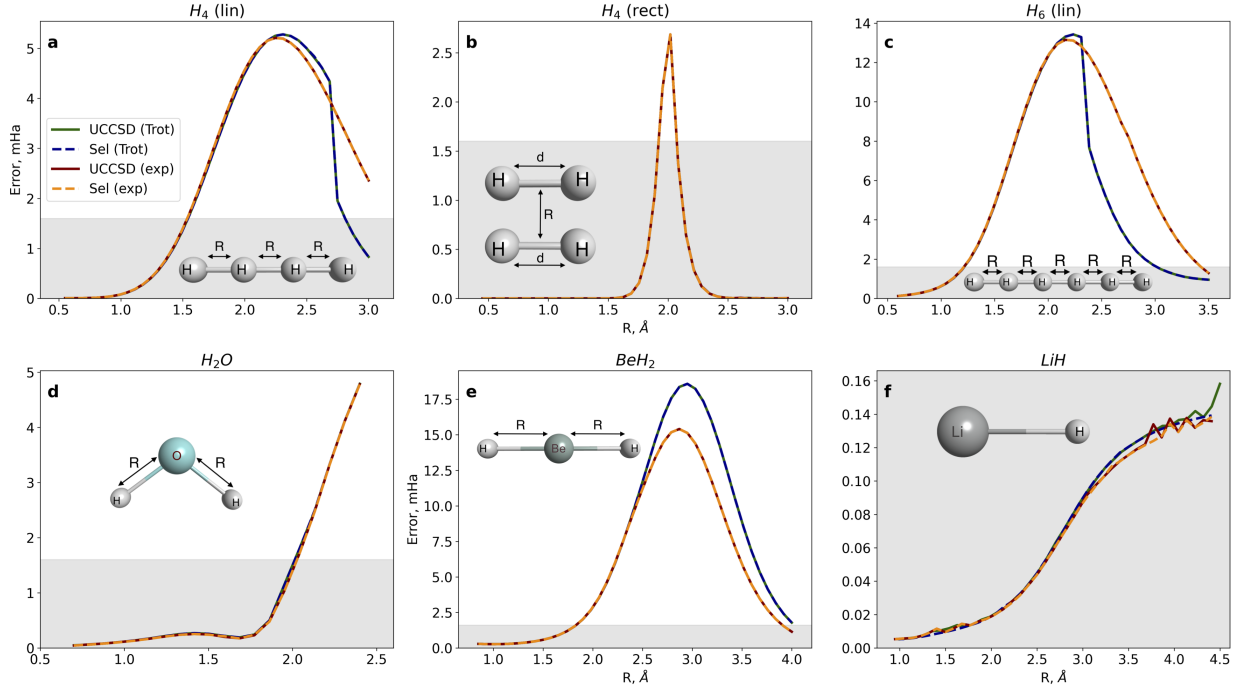


Figure 3: Energy errors w.r.t. FCI of the VQE simulations using full UCCSD ansatz (solid lines) and the prescreened UCCSD ansatz (dashed lines) for a set of symmetric molecules. Green and blue lines correspond to simulations performed by using Trotterization with a single step, and red and orange lines represent the simulations using cluster operator exponentiation.

Table 1: Number of parameters and maximum energy errors for the symmetric geometries of molecules.

Molecule	N parameters		Max error, mHa	
	UCCSD	Screened	Exp	Trot
LiH	92	34	0.0100	0.0013
H ₄ (Lin)	26	14	0.0066	0.0232
H ₄ (Rect)	26	10	0.0054	0.0046
H ₆ (Lin)	117	59	0.0013	0.0909
H ₂ O	140	48	0.0106	0.0103
BeH ₂	204	38	0.0067	0.0088

unimportant single- and double-electron excitations that are present in symmetric molecules without sacrificing accuracy. In fact, on noisy devices, the smaller depth of a circuit with fewer excitation operators will improve accuracy compared with the full UCCSD circuit. When the symmetry is broken, more electron configurations become significant, and consequently more excitations operators have to be included in the UCCSD ansatz. Thus, the ansatz constructed for symmetric configuration can become a poor approximation for the same molecule but in a slightly distorted configuration. Reduction of the number of excitations might not be possible in such a case without the error increase. The electron integral prescreening approach is superior to MP2 screening in getting rid of excitations of negligible amplitudes because it has virtually zero cost compared with N^5 scaling of MP2. Additionally, it works for single excitations. However, MP2 is likely to provide a better relative magnitude of the important amplitudes and work better for non-symmetric cases. At the same time, MP2 amplitudes for some systems might be a poor approximation to CCSD amplitudes, and therefore the prescreening procedure will be inefficient.

While this manuscript was in preparation, Cao et al.⁵⁸ published a study where they suggest a procedure for screening operators for UCCSD by directly applying point group symmetries. We believe this method chooses the same amplitudes as our approach. When the electronic Hamiltonian matrix elements connecting molecular orbitals are zero because of the symmetries, the cluster amplitudes connecting these orbitals are also zero because of the same symmetries.

Many molecules require higher than second-order excitations, including the small molecules depicted in Figure 3 when the bonds are stretched. In the following section, we describe how electron integrals can be used for screening higher-order excitations.

Unitary Selective Coupled Cluster

The USCC method we propose is an iterative method to construct a unitary coupled-cluster ansatz, where the excitation operators are added to the ansatz based on the screening crite-

tion:

$$|H_{ia}t_i| \geq \epsilon. \tag{11}$$

In Equation (11), t_i are the amplitudes corresponding to the excitation operators already included in the ansatz (and determined by VQE optimization). Similarly to the selected CI method (see Eq. (10)), H_{ia} are the electronic Hamiltonian matrix elements h_1 and h_2 connecting the spin orbitals involved in excitations from the reference state defined by amplitudes t_i and t_a . This criterion is inspired by the SHCI criterion, replacing the determinantal coefficient c_i with the cluster amplitude t_i . A first-order expansion of the UCC operator leads to the rough approximation $c_i \approx t_i$. This can be observed in small systems for which there is a one-to-one mapping between determinants and cluster excitation operators; that is, for a certain determinant there is only one excitation operator that connects it to the Hartree–Fock state. In such a case cluster amplitude is equal to the CI coefficient, for example in the H_2 molecule in the minimal basis set. Another way to look at the unitary selective coupled-cluster selection criterion, Equation (11), is that when $t_i \approx 0$, the Trotter step corresponding to that cluster amplitude is nearly identity, meaning that it has little effect on the wave function, although care must be taken because of the periodic nature of the UCC form.

The ansatz generation starts with the reference Hartree–Fock state, and none of the excitation amplitudes are available. First, all possible single- and double-electronic excitations are generated. The first iteration $n = 1$ represents the single- and double-excitation operator prescreening procedure described in the preceding section. All $[i, a]$ and $[i, j, a, b]$ excitations, for which the absolute values of corresponding $h_1[i, a]$ and $h_2[i, j, a, b]$ matrix elements are larger than the threshold value for the first iteration ϵ_1 , are included in the ansatz. Then, this initial ansatz is used to run the first VQE simulation. All $t_1[i, a]$ and $t_2[i, j, a, b]$ amplitudes are saved for future iterations. Thus, each single (double) excitation has two coefficients associated with it, h_1 and t_1 (h_2 and t_2).

After the first iteration, triple and quadruple excitations can be generated from the singles and doubles that are already included in the ansatz. There are multiple ways to

obtain the coefficients in Equation 11 for these higher-order excitations. For example, by cycling through all single excitations $[i, a]$ present in the ansatz we can generate coefficients $t_1[i, a]h_2[j, k, b, c]$ with all possible doubles (already present in the ansatz or not). In addition, the coefficients $h_1[i, a]t_2[j, k, b, c]$ can be generated between singles and doubles present in the ansatz. Also, one can cycle through all doubles present in the ansatz to compute $t_2[i, j, a, b]h_1[k, c]$ coefficients, along with $h_2[i, j, a, b]t_1[k, c]$. All the coefficients mentioned above are associated with triple excitation $[i, j, k, a, b, c]$. Similarly, the coefficients describing quadruples $[i, j, k, l, a, b, c, d]$ include $t_2[i, j, a, b]h_2[k, l, c, d]$ and all variations of indices involved.

During each iteration n , starting from $n = 2$, once all coefficients are computed for all excitations, the largest coefficient associated with an excitation is compared with the ϵ_n value corresponding to the current iteration. The ϵ_n for each iteration can be obtained from a predefined set of values or computed from the previous iteration, for example, $\epsilon_n = \epsilon_{n-1}/2$. A lower ϵ value results in more excitations being included in the ansatz, and the limit of $\epsilon = 0$ corresponds to the full UCC ansatz, including all possible excitations up to desired order. Excitations for which the largest coefficient is larger than ϵ_n are added to the ansatz. In addition to triples and quadruples, it can include the singles and doubles that were not added during the first iteration. After the ansatz is constructed, the first VQE simulation is performed. If the set of excitations does not change from one iteration to another, the algorithm skips to the next ϵ value to avoid repeating the VQE energy evaluation. An alternative way to grow the ansatz is to arrange operators in decreasing order at each iteration so that a constant number of operators with the largest coefficients can be added at each iteration. This iterative procedure is repeated until the termination condition. The latter can be reaching an ϵ value or a standard energy convergence criterion when the energy change between two iterations is smaller than the predefined ϵ_E value. In this paper, we restrict ourselves to including only up to quadruple excitations; in general, this process can be used to select cluster operators of any order, which could be important for larger and

more correlated systems.

Algorithm 1 Unitary Selective Coupled Cluster

Generate single and double excitations for a given molecule.

Initialize an empty ansatz.

Step 1. For all single and double excitations $[i, a]$ and $[i, j, a, b]$ in UCCSD add to ansatz all excitations for which $h_1[i, a]$ and $h_2[i, j, a, b]$ are larger than ϵ_1 .

Repeat until termination condition:

Step 2. Run VQE with the current ansatz to compute energy, update amplitudes for each excitation present in ansatz.

Step 3. For each single $[i, a]$ or double $[i, j, a, b]$ excitation present in ansatz using t_1 and t_2 values from the previous iteration and additional excitations $[k, c]$ or $[k, l, c, d]$ generate triple and quadruple excitations with the following coefficients:

$$\begin{aligned} & t_1[i, a] \cdot h_2[j, k, b, c] \\ & h_1[i, a] \cdot t_2[j, k, b, c] \\ & t_2[i, j, a, b] \cdot h_1[k, c] \\ & h_2[i, j, a, b] \cdot t_1[k, c] \\ & t_2[i, j, a, b] \cdot h_2[k, l, c, d] \end{aligned}$$

Step 4. For each excitation, if the absolute value of the largest coefficient computed in step 3 is larger than ϵ_n on iteration n , add this excitation to ansatz.

Computational Details

All calculations for this work were performed by using Python code that we developed. All required electronic structure calculations on a classical computer, such as computation of one- and two-electron integrals, were performed in the PySCF package v. 1.7.6.⁵⁹ The VQE simulations were performed by using the Qiskit-nature package v. 0.1.3.⁶⁰ To map fermions to qubits, we used Jordan-Wigner mapping.⁴³ The VQE simulations in Qiskit were performed by using the state vector simulator and SLSQP optimizer for finding the classical parameters. A minimal STO-3G basis set was used for all simulations unless explicitly stated otherwise. For all molecules, no molecular orbitals were frozen.

Unitary Selective Coupled Cluster Simulations

We tested our iterative unitary selective coupled-cluster method on the H_6 , H_2O , and BeH_2 set of molecules. Both symmetric and slightly distorted geometries were considered. To showcase the performance of the method in different regions of PESs, we chose three internuclear distances for each molecule: single, double, and triple equilibrium distances. All results were obtained by using cluster operator exponentiation. The USCCSDTQ energy convergence with respect to the number of parameters is depicted in Figure 4 with symmetric geometries in the top row and non-symmetric in the bottom. Each point corresponds to the parameter ϵ reduced by a factor of 2 from the previous iteration. Grey represents the area with errors smaller than chemical accuracy.

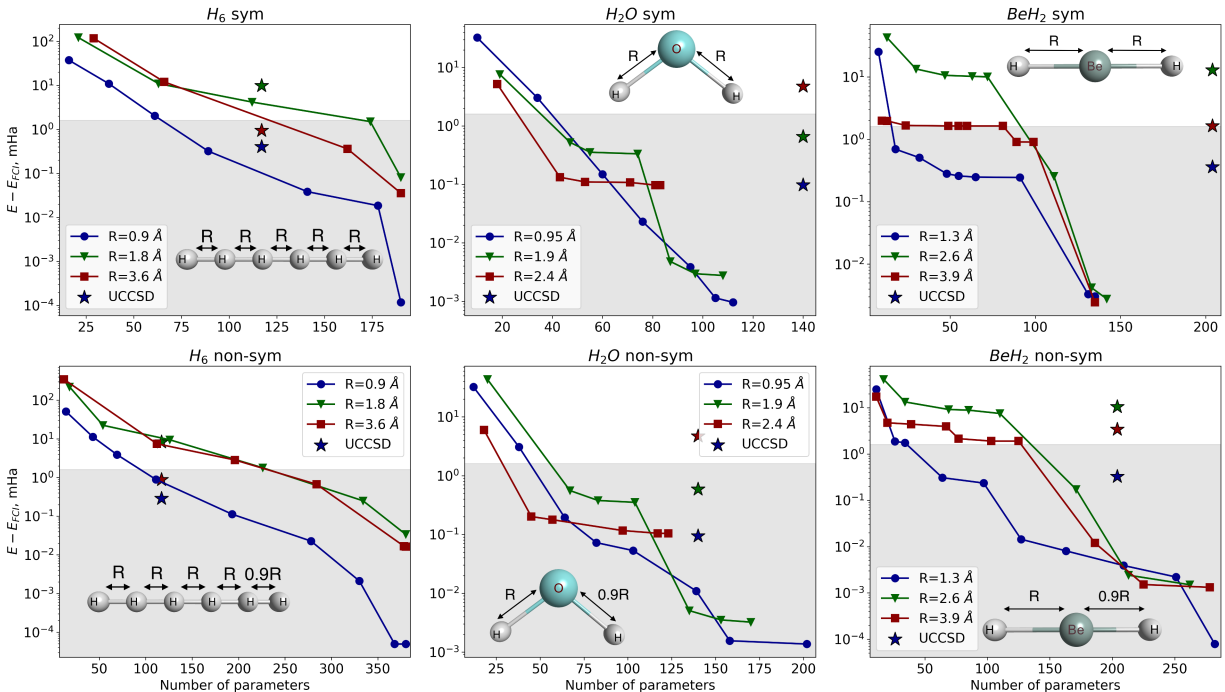


Figure 4: Error of the USCC simulation with respect to the number of parameters in the ansatz for symmetric (top row) and non-symmetric (bottom row) geometries of the H_6 , H_2O , and BeH_2 molecules. Colors represent the internuclear distances. UCCSD results are marked with stars. Each circle corresponds to a data point from each USCC iteration. Grey represents the area with errors smaller than chemical accuracy.

H₆

H₆ is a good benchmarking molecule that has a large pool of possible electronic excitations, especially of order higher than doubles. The standard UCCSD ansatz contains 117 excitations, 18 singles and 99 doubles. For the linear symmetric configuration of H₆ molecule with $R = 2R_{eq} = 1.8 \text{ \AA}$, the UCCSD error with respect to FCI is significantly above the chemical accuracy threshold for both symmetric (9.83 mHa) and non-symmetric (8.26 mHa) configurations (left column in Figure 4). Thus, reducing the error below the chemical accuracy threshold requires excitations of higher orders. When triples and quadruples are added, the error becomes below the chemical accuracy threshold to 1.51 mHa with 174 operators. Out of 174 excitation operators, 68 are triples and 47 quadruples, each of which has a relatively small contribution to the correlation energy. However, triples and quadruples are required in order to reach chemical accuracy. Although these higher-order excitations are costly in terms of gate count, the number of such excitations is significantly smaller than the total number of possible triple and quadruple excitations, 164 and 99, respectively. In addition, our method provides a systematic way to improve the accuracy through the addition of operators that are more likely to contribute.

At single and triple equilibrium distances, fewer excitations are needed to achieve high accuracy. For the symmetric configuration with $R = R_{eq} = 0.9 \text{ \AA}$ the 0.32 mHa error is achieved by using 89 parameters, which is comparable to the UCCSD error. At $R = 3R_{eq} = 3.6 \text{ \AA}$ the error is below chemical accuracy at 0.12 mHa, with 66 parameters compared with 0.9 mHa error obtained with UCCSD.

The non-symmetric configuration of the H₆ molecule has a much larger number of significant excitations (see bottom left panel Figure 4). USCCSDTQ performs better at equilibrium distance, achieving 0.89 mHa error with 111 operators. The UCCSD error is 0.29 mHa with 117 operators. At $R = 3R_{eq} = 3.6 \text{ \AA}$ the UCCSD error is within chemical accuracy and provides better results than USCCSDTQ with fewer operators. This shows the limitations of our method, specifically the crude approximation for the screening coefficient computation,

which can become unreliable in a system with a large number of excitations, each contributing little to correlation energy. At $R = 2R_{eq} = 1.8 \text{ \AA}$ the USCCSDTQ also requires more operators to achieve accuracy comparable to that of UCCSD. However, the UCCSD error is large, 8.3 mHa, and our method allows adding more operators to reduce the error. The USCCSDTQ simulation error with 334 parameters is 0.25 mHa, and the previous iteration with 226 operators gets close to the chemical accuracy threshold with 1.78 mHa error.

This system demonstrates that it is much more challenging to study highly correlated systems outside equilibrium geometries and when the symmetry is broken.

H₂O

At $R = 0.95 \text{ \AA}$ and $R = 2.4 \text{ \AA}$ UCCSD errors for both symmetric and non-symmetric configurations of the H₂O molecule are within chemical accuracy (see center column of Figure 4). For the symmetric configuration at $R = 0.95 \text{ \AA}$, around the equilibrium geometry, the UCCSD error is 0.10 mHa with 140 parameters, whereas the USCCSDTQ error is 0.14 mHa using 60 parameters. For the non-symmetric configuration, the UCCSD error is 0.10 mHa, whereas the USCCSDTQ error is 0.19 mHa with 64 parameters. For the symmetric configuration at $R = 1.9 \text{ \AA}$ the UCCSD error is 0.65 mHa, and the USCCSDTQ error reaches 0.53 mHa accuracy with 47 parameters. UCCSD for the non-symmetric configuration has an error of 0.59 mHa, and USCCSDTQ reaches 0.56 mHa accuracy with 67 parameters. Overall our method achieves accuracy that is comparable to or better than that of UCCSD with a smaller number of parameters. At $R = 2.4 \text{ \AA}$ for the symmetric configuration of H₂O, the UCCSD error with 140 parameters is above the chemical accuracy threshold, 5.2 mHa, whereas our method achieves an error of 0.13 mHa only using 43 operators with 14 triples and 3 quadruples. The UCCSD for a non-symmetric configuration at the same internuclear separation has an error of 6.01 mHa, whereas USCCSDTQ requires 45 operators to achieve 0.20 mHa accuracy, with 14 triples and 3 quadruples.

BeH₂

The UCCSD ansatz BeH₂ molecule contains 204 operators. For the symmetric configuration at $R = R_{eq} = 1.3 \text{ \AA}$ the UCCSD energy is within chemical accuracy with an error of 0.36 mHa (0.36 mHa using Trotterization with a single step). The energy obtained by using our USCCSDTQ algorithm is 0.69 mHa with only 18 operators (6 singles and 12 doubles; see the top right panel of Figure 4). With 48 operators, the energy reaches the accuracy obtained with UCCSD.

The UCCSD error at $R = 2R_{eq} = 2.6 \text{ \AA}$ is 12.94 mHa (14.01 mHa using Trotterization with a single step), which means that to obtain a quantitatively accurate PES, higher-order excitations are required. Our method requires around 50 operators to achieve accuracy comparable to that of UCCSD, and 111 operators are needed to achieve an error below the chemical accuracy threshold (0.26 mHa).

At $R = 3R_{eq} = 3.9 \text{ \AA}$ the UCCSD error is around chemical accuracy, 1.63 mHa (2.56 mHa using Trotterization with a single step), which is achieved by our method with 49 operators. There is a region where the error is flat with the increasing number of operators added to ansatz. This means that some unimportant operators are being added to the ansatz ahead of the ones that reduce the energy in later iterations. This shows some limitations of our method. When the magnitudes of the amplitudes for different excitations are similar, which is the case for this stretched geometry, the coefficients we compute with the USCC method can become a poor approximation for choosing the important UCC amplitudes.

For the non-symmetric geometries (bottom right panel of Figure 4), the UCCSD errors are in general higher, and only the $R = R_{eq}$ point is within chemical accuracy. For $R = R_{eq} = 1.3 \text{ \AA}$ our method achieves chemical accuracy, 0.31 mHa error, with 64 operators instead of 204. For $R = 2R_{eq}$ chemical accuracy is achieved by using 171 operators with an error of 0.17 mHa. At $R = 3R_{eq}$ the error is 0.01 mHa with 186 operators.

Although the number of operators in both symmetric and non-symmetric configurations is large, it is significantly lower than the 1,064 operators that constitute the full UCCSDTQ

ansatz.

Discussion

For all molecules studied in this work, the symmetric geometries have significantly fewer electron configurations contributing to the wave function. As a result, convergence to the exact solution requires fewer excitation operators in the ansatz. Because of hardware limitations, the simulations were run only for the minimal basis set. Figure 5 shows that our prescreening method is even more beneficial when larger basis sets are used. The ratio of important operators decreases with the increasing basis set for all studied molecules for both symmetric and non-symmetric configurations. The most profound reduction is observed for the non-symmetric configurations of the H_4 and H_6 molecules, for which in the minimal basis set none of the operators are negligible.

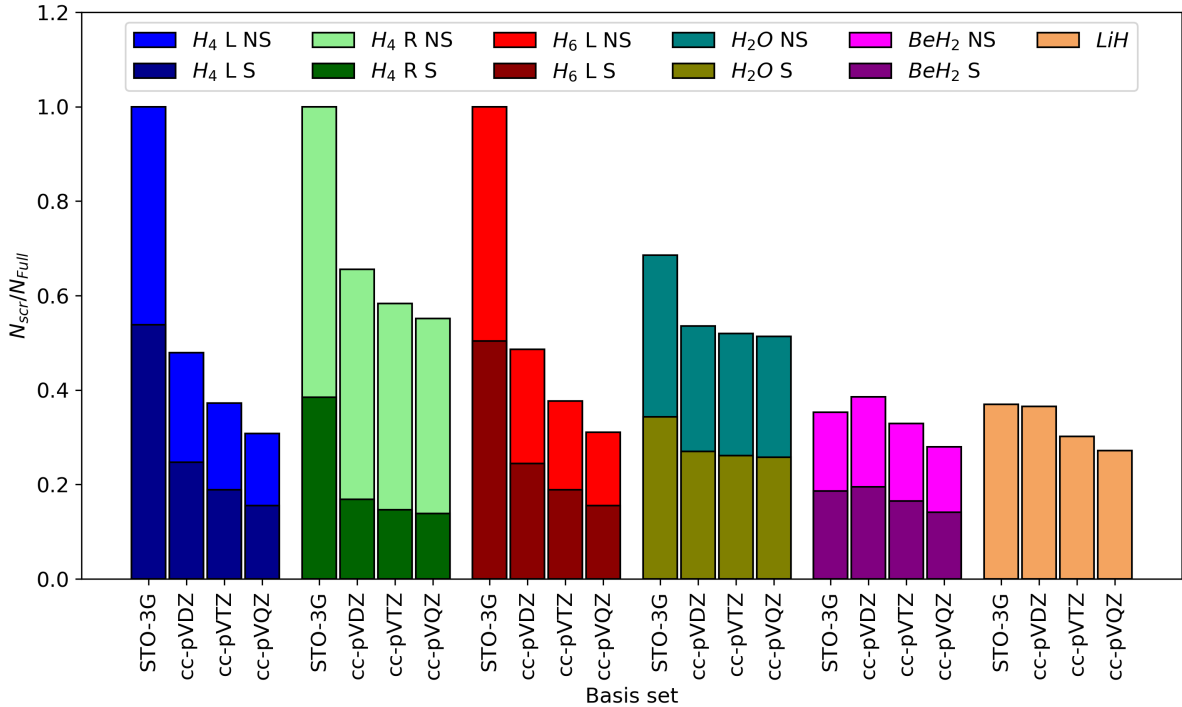


Figure 5: Ratios of the number of operator in prescreened ansatz to the number of the operators in full UCCSD ansatz for a set of symmetric and non-symmetric geometry of molecules: linear (L) H_4 , rectangular (R) H_4 , linear (L) H_6 , BeH_2 , LiH . S corresponds to the symmetric geometry, and NS corresponds to non-symmetric geometry.

Although the gate cost of implementing triple and quadruple excitations on quantum computers is high, our proposed method offers a systematic and inexpensive way to expand the UCC ansatz to improve accuracy. When comparing our USCC algorithm with adaptive methods such as ADAPT-VQE, we note that ADAPT-VQE will always construct a more compact ansatz because at every iteration it computes the energy gradients with respect to variational parameters for every element in the operator pool. The cost of such computations can be estimated as the measurement for up to N^4 Hamiltonian terms multiplied by the number of operators in the pool. The measurements of gradients for each variational parameter can be performed simultaneously because they are independent. For larger systems, however, the total cost in terms of shots can become infeasible. The USCC method has longer circuits but a much smaller shot count. A possible way to reduce the gate count is to use the qubit excitations instead of fermionic excitations.³⁵ The cost of implementing qubit excitations is constant with respect to the number of qubits, which can dramatically reduce the gate count. However, ansatzes consisting of such excitations do not preserve the antisymmetry of the electronic wave function. Although such an approach has been shown to work for small molecules, studies for larger molecules are needed in order to definitively conclude that such an approach is scalable.

Most methods for VQE simulations derive building blocks for ansatz construction from the fermionic excitations and do not go beyond double excitations because of the high cost. This cost comes not just from the large number of gates required to implement each triple or quadruple excitation but also because the total number of such operators also grows quickly. To compensate for the lack of higher-order excitations, one can use the UCCSD ansatz with generalized singles and doubles excitations (UCCGSD).⁶¹ In UCCGSD, excitations are generated between all orbitals, including virtual-virtual and occupied-occupied combinations. It allows one to recover more correlation energy than the standard UCCSD does. The number of such generalized excitations, however, grows much faster than standard UCCSD. To reduce the cost, the k -UpCCGSD method uses only pair double excitations in the ansatz

and increases the flexibility of the ansatz by using k repetitions of the circuit. In the ADAPT-VQE method, only operators that contribute to correlation energy are added to the ansatz. The operator that will contribute the most to the correlation energy is picked based on the gradient of energy with respect to the variational parameter.²³ The cost of computing gradients for such a large operator pool will result in a very high total shot count. We expect that the screening procedure based on the electron integrals described in Section Fermionic Operator Prescreening of this paper can be used to reduce the size of the ADAPT-VQE pool. This will be the focus of our future work. Additionally, the same screening procedure can be applied for constructing a more compact k-UpCCGSD ansatz without accuracy loss, or even k-UCCGSD, where all prescreened double excitations would be included, not just pair doubles.

In this work, we have shown that the symmetry in molecules has a strong impact on the number of electron configurations contributing to the wave function. For systems with broken symmetry, a much larger number of excitations has to be included in the ansatz. The less symmetric a molecule is, the larger the number of non-negligible excitations will be, as is demonstrated by Cao et al.⁵⁸ based on point group symmetries. In most studies describing new methods for constructing compact ansatzes for VQE simulations, the test molecules have a symmetric geometric configuration. We suggest that the performance of such truncated ansatzes should be tested against non-symmetric molecules as well, because the performance of such ansatzes might significantly depend on the geometry, unlike the complete ansatz, for example, UCCSD, which contains all possible excitations, and the performance difference between symmetric and non-symmetric systems is much less profound. In cases of symmetric molecules, we believe that our prescreening method can significantly reduce the computational cost of most UCC-based existing methods, with negligible overhead.

Conclusions

We have proposed a method to prescreen single and double fermionic excitations when constructing a unitary coupled-cluster ansatz for molecular systems. By removing the excitations that connect the orbitals for which one- and two-electron integrals are zero, one can dramatically reduce the size of ansatz without any loss in accuracy and with essentially zero overhead. The reduction in the number of excitations is most significant for highly symmetric molecules, such as BeH_2 , where the number of excitations is reduced by a factor of 5 using just a minimal basis set. We have shown that with increasing basis set size the ratio of unimportant excitations grows, and our proposed screening procedure becomes even more beneficial. The most important advantage of this procedure is the essentially zero computational cost, which requires just a look-up of electronic Hamiltonian matrix elements, which are precomputed before any quantum chemistry simulation, including VQE.

To construct unitary coupled cluster ansatz with arbitrary order excitations, we proposed the selective coupled-cluster algorithm. At each iteration, it uses the amplitudes of the excitations already included in ansatz and the values of the electronic Hamiltonian matrix elements to find important excitations of higher order to include in the ansatz. On a test set of small molecules, we have shown that it systematically improves accuracy at each iteration. However, it has limitations, for example at larger internuclear distances, where many electron configurations have contributions to the wave function similar in magnitude. In future work, the method can be improved by utilizing a less crude approximation for the coefficients that define the importance of each excitation. This improvement can potentially be achieved by using perturbation theory when computing these “importance coefficients,” as is done in some flavors of selected CI. The current use of just electronic Hamiltonian matrix elements and cluster amplitudes from previous iterations serves as a proof of concept and is a crude approximation to demonstrate the potential of such an approach.

Acknowledgement

This material is based upon work supported by the U.S. Department of Energy, Office of Science, Office of Fusion Energy Sciences, under Award Number DE-SC0020249. Y.A.'s work at Argonne National Laboratory was supported by the U.S. Department of Energy, Office of Science, under contract DE-AC02-06CH11357. This work was performed, in part, at the Center for Nanoscale Materials, a U.S. Department of Energy Office of Science User Facility, and supported by the U.S. Department of Energy, Office of Science, under Contract No. DE-AC02-06CH11357.

References

- (1) Kitaev, A. Y. Quantum measurements and the Abelian Stabilizer Problem. *arXiv* **1995**,
- (2) Abrams, D. S.; Lloyd, S. Simulation of Many-Body Fermi Systems on a Universal Quantum Computer. *Phys. Rev. Lett.* **1997**, *79*, 2586–2589.
- (3) Abrams, D. S.; Lloyd, S. Quantum Algorithm Providing Exponential Speed Increase for Finding Eigenvalues and Eigenvectors. *Phys. Rev. Lett.* **1999**, *83*, 5162–5165.
- (4) Preskill, J. Quantum Computing in the NISQ era and beyond. *Quantum* **2018**, *2*, 79.
- (5) Elfving, V. E.; Broer, B. W.; Webber, M.; Gavartin, J.; Halls, M. D.; Lorton, K. P.; Bochevarov, A. How will quantum computers provide an industrially relevant computational advantage in quantum chemistry? *arXiv preprint arXiv:2009.12472* **2020**,
- (6) Peruzzo, A.; McClean, J.; Shadbolt, P.; Yung, M.-H.; Zhou, X.-Q.; Love, P. J.; Aspuru-Guzik, A.; O'Brien, J. L. A variational eigenvalue solver on a photonic quantum processor. *Nature Communications* **2014**, *5*, 4213.
- (7) Fedorov, D. A.; Peng, B.; Govind, N.; Alexeev, Y. VQE Method: A Short Survey and Recent Developments. **2021**,

- (8) Taube, A. G.; Bartlett, R. J. New perspectives on unitary coupled-cluster theory. *Int. J. Quantum Chem.* **2006**, *106*, 3393–3401.
- (9) Evangelista, F. A.; Chan, G. K.-L.; Scuseria, G. E. Exact parameterization of fermionic wave functions via unitary coupled cluster theory. *J. Chem. Phys.* **2019**, *151*, 244112.
- (10) Cooper, B.; Knowles, P. J. Benchmark studies of variational, unitary and extended coupled cluster methods. *J. Chem. Phys.* **2010**, *133*, 234102.
- (11) Harsha, G.; Shiozaki, T.; Scuseria, G. E. On the difference between variational and unitary coupled cluster theories. *J. Chem. Phys.* **2018**, *148*, 044107.
- (12) Pal, S. Use of a unitary wavefunction in the calculation of static electronic properties. *Theo. Chim. Acta* **1984**, *66*, 207–215.
- (13) McClean, J. R.; Romero, J.; Babbush, R.; Aspuru-Guzik, A. The theory of variational hybrid quantum-classical algorithms. *New J. Phys.* **2016**, *18*, 023023.
- (14) Romero, J.; Babbush, R.; McClean, J. R.; Hempel, C.; Love, P. J.; Aspuru-Guzik, A. Strategies for quantum computing molecular energies using the unitary coupled cluster ansatz. *Quantum Science and Technology* **2018**, *4*, 014008.
- (15) Kandala, A.; Mezzacapo, A.; Temme, K.; Takita, M.; Brink, M.; Chow, J. M.; Gambetta, J. M. Hardware-efficient variational quantum eigensolver for small molecules and quantum magnets. *Nature* **2017**, *549*, 242–246.
- (16) Kandala, A.; Temme, K.; Córcoles, A. D.; Mezzacapo, A.; Chow, J. M.; Gambetta, J. M. Error mitigation extends the computational reach of a noisy quantum processor. *Nature* **2019**, *567*, 491–495.
- (17) Barkoutsos, P. K.; Gonthier, J. F.; Sokolov, I.; Moll, N.; Salis, G.; Fuhrer, A.; Ganzhorn, M.; Egger, D. J.; Troyer, M.; Mezzacapo, A.; Filipp, S.; Tavernelli, I. Quan-

- tum algorithms for electronic structure calculations: Particle-hole Hamiltonian and optimized wave-function expansions. *Physical Review A* **2018**, *98*, 022322.
- (18) Ganzhorn, M.; Egger, D.; Barkoutsos, P.; Ollitrault, P.; Salis, G.; Moll, N.; Roth, M.; Fuhrer, A.; Mueller, P.; Woerner, S.; Tavernelli, I.; Filipp, S. Gate-Efficient Simulation of Molecular Eigenstates on a Quantum Computer. *Phys. Rev. Applied* **2019**, *11*, 044092.
- (19) Gard, B. T.; Zhu, L.; Barron, G. S.; Mayhall, N. J.; Economou, S. E.; Barnes, E. Efficient symmetry-preserving state preparation circuits for the variational quantum eigensolver algorithm. *npj Quantum Information* **2020**, *6*, 10.
- (20) McClean, J. R.; Boixo, S.; Smelyanskiy, V. N.; Babbush, R.; Neven, H. Barren plateaus in quantum neural network training landscapes. *Nature Communications* **2018**, *9*, 4812.
- (21) Wang, S.; Fontana, E.; Cerezo, M.; Sharma, K.; Sone, A.; Cincio, L.; Coles, P. J. Noise-Induced Barren Plateaus in Variational Quantum Algorithms. **2021**,
- (22) Cerezo, M.; Sone, A.; Volkoff, T.; Cincio, L.; Coles, P. J. Cost function dependent barren plateaus in shallow parametrized quantum circuits. *Nature Communications* **2021**, *12*, 1791.
- (23) Grimsley, H. R.; Economou, S. E.; Barnes, E.; Mayhall, N. J. An adaptive variational algorithm for exact molecular simulations on a quantum computer. *Nature Communications* **2019**, *10*, 3007.
- (24) Tang, H. L.; Shkolnikov, V.; Barron, G. S.; Grimsley, H. R.; Mayhall, N. J.; Barnes, E.; Economou, S. E. Qubit-ADAPT-VQE: An Adaptive Algorithm for Constructing Hardware-Efficient Ansätze on a Quantum Processor. *PRX Quantum* **2021**, *2*, 020310.

- (25) Ryabinkin, I. G.; Yen, T.-C.; Genin, S. N.; Izmaylov, A. F. Qubit Coupled Cluster Method: A Systematic Approach to Quantum Chemistry on a Quantum Computer. *Journal of Chemical Theory and Computation* **2018**, *14*, 6317–6326.
- (26) Ryabinkin, I. G.; Lang, R. A.; Genin, S. N.; Izmaylov, A. F. Iterative Qubit Coupled Cluster Approach with Efficient Screening of Generators. *Journal of Chemical Theory and Computation* **2020**, *16*, 1055–1063.
- (27) Lang, R. A.; Ryabinkin, I. G.; Izmaylov, A. F. Unitary transformation of the electronic Hamiltonian with an exact quadratic truncation of the Baker–Campbell–Hausdorff expansion. **2020**,
- (28) Claudino, D.; Wright, J.; McCaskey, A. J.; Humble, T. S. Benchmarking Adaptive Variational Quantum Eigensolvers. *Frontiers in Chemistry* **2020**, *8*, 1152.
- (29) Sim, S.; Romero, J.; Gonthier, J. F.; Kunitsa, A. A. Adaptive pruning-based optimization of parameterized quantum circuits. **2020**,
- (30) Mazziotti, D. A. Exactness of wave functions from two-body exponential transformations in many-body quantum theory. *Phys. Rev. A* **2004**, *69*, 012507.
- (31) Mazziotti, D. A. Exact two-body expansion of the many-particle wave function. *Phys. Rev. A* **2020**, *102*, 030802.
- (32) Mazziotti, D. A. Anti-Hermitian Contracted Schrödinger Equation: Direct Determination of the Two-Electron Reduced Density Matrices of Many-Electron Molecules. *Phys. Rev. Lett.* **2006**, *97*, 143002.
- (33) Mazziotti, D. A. Anti-Hermitian part of the contracted Schrödinger equation for the direct calculation of two-electron reduced density matrices. *Phys. Rev. A* **2007**, *75*, 022505.

- (34) Mukherjee, D.; Kutzelnigg, W. Irreducible Brillouin conditions and contracted Schrödinger equations for n-electron systems, I: The equations satisfied by the density cumulants. *J. Chem. Phys.* **2001**, *114*, 2047–2061.
- (35) Yordanov, Y. S.; Arvidsson-Shukur, D. R. M.; Barnes, C. H. W. Efficient quantum circuits for quantum computational chemistry. *Physical Review A* **2020**, *102*.
- (36) Yordanov, Y. S.; Armaos, V.; Barnes, C. H. W.; Arvidsson-Shukur, D. R. M. Iterative qubit-excitation based variational quantum eigensolver. *arXiv* **2020**,
- (37) Head-Gordon, M.; Pople, J. A.; Frisch, M. J. MP2 energy evaluation by direct methods. *Chemical Physics Letters* **1988**, *153*, 503–506.
- (38) Møller, C.; Plesset, M. S. Note on an Approximation Treatment for Many-Electron Systems. *Physical Review* **1934**, *46*, 618–622.
- (39) McArdle, S.; Endo, S. Quantum computational chemistry. *Rev. Mod. Phys.* **2020**, *92*, 015003.
- (40) Cao, Y.; Romero, J.; Olson, J. P.; Degroote, M.; Johnson, P. D.; Kieferova, M.; Kivlichan, I. D.; Menke, T.; Peropadre, B.; Sawaya, N. P. D.; Sim, S.; Veis, L.; Aspuru-Guzik, A. Quantum Chemistry in the Age of Quantum Computing. *Chem. Rev.* **2019**, *119*, 10856–10915.
- (41) Cerezo, M.; Arrasmith, A.; Babbush, R.; Benjamin, S. C.; Endo, S.; Fujii, K.; McClean, J. R.; Mitarai, K.; Yuan, X.; Cincio, L.; Coles, P. J. Variational quantum algorithms. *arXiv* **2020**,
- (42) Bharti, K.; Cervera-Lierta, A.; Kyaw, T. H.; Haug, T.; Alperin-Lea, S.; Anand, A.; Degroote, M.; Heimonen, H.; Kottmann, J. S.; Menke, T.; Mok, W.-K.; Sim, S.; Kwek, L.-C.; Aspuru-Guzik, A. Noisy intermediate-scale quantum (NISQ) algorithms. **2021**,

- (43) Jordan, P.; Wigner, E. Über das Paulische Äquivalenzverbot. *Z. Phys.* **1928**, *47*, 631–651.
- (44) McClean, J. R.; Babbush, R.; Love, P. J.; Aspuru-Guzik, A. Exploiting Locality in Quantum Computation for Quantum Chemistry. *J. Phys. Chem. Lett.* **2014**, *5*, 4368–4380.
- (45) Purvis, G. D.; Bartlett, R. J. A full coupled-cluster singles and doubles model: The inclusion of disconnected triples. *The Journal of Chemical Physics* **1982**, *76*, 1910–1918.
- (46) Hatano, N.; Suzuki, M. Finding Exponential Product Formulas of Higher Orders. *Lecture Notes in Physics* **2005**, 37–68.
- (47) O’Malley, P. J. J. et al. Scalable Quantum Simulation of Molecular Energies. *Phys. Rev. X* **2016**, *6*, 031007.
- (48) Knowles, P. J.; Handy, N. C. A new determinant-based full configuration interaction method. *Chemical Physics Letters* **1984**, *111*, 315–321.
- (49) Pople, J.; Seeger, R.; Krishnan, R. Variational configuration interaction methods and comparison with perturbation theory. *International Journal of Quantum Chemistry* **1977**, *12*, 149–163.
- (50) Evangelisti, S.; Daudey, J.-P.; Malrieu, J.-P. Convergence of an improved CIPSI algorithm. *Chemical Physics* **1983**, *75*, 91–102.
- (51) Tubman, N. M.; Lee, J.; Takeshita, T. Y.; Head-Gordon, M.; Whaley, K. B. A deterministic alternative to the full configuration interaction quantum Monte Carlo method. *The Journal of Chemical Physics* **2016**, *145*, 044112.
- (52) Holmes, A. A.; Tubman, N. M.; Umrigar, C. Heat-bath configuration interaction: An efficient selected configuration interaction algorithm inspired by heat-bath sampling. *Journal of Chemical Theory and Computation* **2016**, *12*, 3674–3680.

- (53) Li, J.; Otten, M.; Holmes, A. A.; Sharma, S.; Umrigar, C. J. Fast semistochastic heat-bath configuration interaction. *The Journal of Chemical Physics* **2018**, *149*, 214110.
- (54) Li, J.; Yao, Y.; Holmes, A. A.; Otten, M.; Sun, Q.; Sharma, S.; Umrigar, C. Accurate many-body electronic structure near the basis set limit: Application to the chromium dimer. *Physical Review Research* **2020**, *2*, 012015.
- (55) Holmes, A. A.; Umrigar, C.; Sharma, S. Excited states using semistochastic heat-bath configuration interaction. *The Journal of Chemical Physics* **2017**, *147*, 164111.
- (56) Chien, A. D.; Holmes, A. A.; Otten, M.; Umrigar, C. J.; Sharma, S.; Zimmerman, P. M. Excited states of methylene, polyenes, and ozone from heat-bath configuration interaction. *The Journal of Physical Chemistry A* **2018**, *122*, 2714–2722.
- (57) Li, J.; Otten, M.; Holmes, A. A.; Sharma, S.; Umrigar, C. J. Fast Semistochastic Heat-Bath Configuration Interaction. *arXiv* **2018**,
- (58) Cao, C.; Hu, J.; Zhang, W.; Xu, X.; Chen, D.; Yu, F.; Li, J.; Hu, H.; Lv, D.; Yung, M.-H. Towards a Larger Molecular Simulation on the Quantum Computer: Up to 28 Qubits Systems Accelerated by Point Group Symmetry. 2021.
- (59) Sun, Q.; Berkelbach, T. C.; Blunt, N. S.; Booth, G. H.; Guo, S.; Li, Z.; Liu, J.; McClain, J. D.; Sayfutyarova, E. R.; Sharma, S.; Wouters, S.; Chan, G. K. P `iscpy/iscpy` SCF: the Python-based simulations of chemistry framework. *WIREs Computational Molecular Science* **2018**, *8*.
- (60) ANIS, M. S. et al. Qiskit: An Open-source Framework for Quantum Computing. 2021.
- (61) Lee, J.; Huggins, W. J.; Head-Gordon, M.; Whaley, K. B. Generalized Unitary Coupled Cluster Wave functions for Quantum Computation. *J. Chem. Theory Comput.* **2018**, *15*, 311–324.